ORNL/Sub/00-43892/01

MODELING OF DIRECT LIQUID INJECTION CHEMICAL VAPOR DEPOSITION FOR THERMAL BARRIER COATINGS

January 15, 2003

Report Prepared by

Thomas L. Starr and Weijie Xu
Chemical Engineering Department
University of Louisville
Louisville, KY 40292

under

UT-Battelle subcontract 4000003892

for

OAK RIDGE NATIONAL LABORATORY

Oak Ridge, Tennessee 37831

Managed by

UT-BATTELLE, LLC

for the

U. S. DEPARTMENT OF ENERGY

under contract DE-AC05-00OR22725

ORNL/Sub/00-43892/01

MODELING OF DIRECT LIQUID INJECTION CHEMICAL VAPOR DEPOSITION FOR THERMAL BARRIER COATINGS

January 15, 2003
Research sponsored by the U. S. Department of Energy,
Office of Fossil Energy
Advanced Research Materials Program
Report Prepared by

Thomas L. Starr and Weijie Xu
Chemical Engineering Department
University of Louisville
Louisville, KY 40292

under
UT-Battelle subcontract 4000003892
for
OAK RIDGE NATIONAL LABORATORY
Oak Ridge, Tennessee 37831
Managed by
UT-BATTELLE, LLC
for the
U. S. DEPARTMENT OF ENERGY
under contract DE-AC05-00OR22725

INTRODUCTION

Thermal barrier coatings are important components of current and future energy systems. Such coatings – applied to hot, metallic surfaces in combustors, heat exchanger and turbines – increase the allowable operating temperature and increase the efficiency of the system. Because of its low thermal conductivity and high thermal expansion yttria-stabilized zirconia (YSZ) is the material of choice for protection of structural components in many high temperature applications. Current coating application methods have their drawbacks, however. Air plasma spray (APS) is a relatively low-cost process and is suitable for large and relatively complex shapes. It is difficult to produce uniform, relatively thin coatings with this process, however, and the coatings do not exhibit the columnar microstructure that is needed for reliable, long-term performance. The electron-beam physical vapor deposition (EB-PVD) process does produce the desirable microstructure, however, the capital cost of these systems is very high and the line-of-sight nature of the process limits coating uniformity and the ability to coat large and complex shapes.

The chemical vapor deposition (CVD) process also produces the desirable columnar microstructure and – under proper conditions – can produce uniform coatings over complex shapes. CVD has been used for many materials but is relatively undeveloped for oxides, in general, and for zirconia, in particular. The overall goal of this project – a joint effort of the University of Louisville and Oak Ridge National Laboratory (ORNL) – is to develop the YSZ CVD process for application of thermal barrier coatings for fossil energy systems. This report describes the modeling effort at the University of Louisville, which supports the experimental work at ORNL.

Early work on CVD of zirconia and yttria used metal chlorides, which react with water vapor to form solid oxide[1,2,3]. Because of this rapid gas-phase reaction the water generally is formed in-situ using the reverse water-gas-shift reaction or a microwave plasma[4,5]. Even with these arrangements gas-phase nucleation and powder formation are problems when using these precursors.

Recent efforts on CVD of zirconia and YSZ have focused on use of metal-organic precursors (MOCVD)[6-10]. These are more stable in the gas-phase and can produce dense, crystalline films. With

Research sponsored by the U.S. Department of Energy, Fossil Energy Advanced Research Materials Program, DOE/FE AA 15 10 10 0

metal-organic CVD, consistent controlled delivery of the precursor vapor is sometimes a problem. Direct vaporization and vapor-phase metering is difficult due to marginal thermal stability of these compounds and changes in vaporization rate over time. A number of special precursor delivery systems have been designed to address these challenges[11-15]. The direct liquid injection (DLI) method has several advantages for precursor delivery. Liquid metering provides accurate, stable control of precursor delivery rate. With a suitable solvent, a wide variety of precursor compounds can be used, including solids and other compounds not suitable for vapor delivery. Composite or multi-metal coatings require only one precursor source consisting of multiple precursors dissolved in the correct proportion in a single solution.

Many uses of DLI-MOCVD involve deposition of thin films for electronic applications. In these applications, the substrate temperature is low and the deposition rate is relatively slow (< 1 μm/hr). Under these conditions the deposition rate is kinetics-limited, i.e. controlled by the rate of reaction of adsorbed species on the substrate surface, and is strongly influenced by temperature. Thermal barrier applications require relatively thick films (50 to 100 μm) and higher deposition rates. At the higher temperatures the deposition rate is "transport-limited", i.e. control by the transport rate of precursor to the surface. The purpose of this study is to investigate the deposition of zirconia under transport-limited conditions and to accurately model the deposition rate. Ultimately this model will be used to design a DLI-MOCVD reactor for coating of large, complex shapes such as turbine blades and vanes for fossil energy systems.

EXPERIMENT AND MODELING METHODS

This investigation includes experimental deposition studies at ORNL and model development at the University of Louisville. Progress reports on this joint investigation have been presented at the annual Fossil Energy Materials Conferences. This report summarizes the experimental work at Oak Ridge and details the modeling results from UofL.

EXPERIMENT

Experimental investigation of the CVD process at ORNL uses a stagnation flow reactor, which is shown schematically in Figure 1 and described in greater detail elsewhere[16]. This system uses metal-organic complexes of zirconium and yttrium as precursors for zirconia and YSZ. In particular, $Zr(tmhd)_4$ and $Y(tmhd)_3$, where tmhd = tetramethylheptanedionate, are dissolved in tetrahydrofuran (THF; C_4H_8O) and delivered in liquid solution to a vaporizing nozzle. A relatively small amount of oxygen also is used as carrier and oxidizer to prevent the formation of carbon deposit.

MODEL DESCRIPTION

This research uses a commercial fluid dynamics code (CFD-ACE from CFD Research Corporation, Huntsville, AL) with an axisymmetric 3-D model for heat, momentum and mass transport throughout the reactor. Detailed reactor geometry and boundary conditions are set to match experiments at ORNL. Kinetics and transport parameters are derived from literature and from comparison to experiments at ORNL. All model runs were under steady-state conditions.

Figure 1 shows the reactor model used to simulate the ORNL reactor. The axisymmetric computational region includes the volume from the outer surfaces of the nozzle (inlet) to a position several centimeters downstream from the substrate surface. In the radial direction the model volume extends from the centerline of the reactor to the inner wall of the quartz reactor tube. All model dimensions are set to match ORNL reactor dimensions. The computational volume is divided into 974 elements with a variable mesh as illustrated.

Constant temperature conditions are used at all boundaries. The nozzle surfaces are set to $200^{o}C$, the controlled temperature of the oil-jacketed nozzle. The substrate and susceptor surfaces are set to the pyrometer-controlled temperature reported for a particular experiment. The outer wall temperature is 100°C, an estimate of actual temperature during a run.

Mass flow boundary conditions are "no-slip" at all solid surfaces, constant velocity across the inlet and "outflow" at the outlet boundary. Inlet gas velocity of 92 cm/s is calculated from the molar flow rate (2.54×10^{-4} mole/s including solution vapor and oxygen), nozzle diameter (2.4 cm) and the ideal gas law at the nozzle temperature and system pressure (2370 Pa).

Species transport boundary conditions are "zero-transport" for all species at the nozzle wall and outer wall and "constant concentration" at the inlet. Inlet gas composition, in mass fractions, is 0.033 $Zr(tmhd)_4$, 0.005 $Y(tmhd)_3$, 0.145 O_2 and 0.817 THF. At the substrate and susceptor surfaces, the species transport in/out of the surface is determined by Arrhenius-type reactions, first-order with respect to the gas-phase concentration of the precursor species at the surface.

$$Zr(tmhd)_4 \rightarrow ZrO_2(s) + 6\ CO + 19\ C_2H_2 \qquad (1a)$$

$$2\ Y(tmhd)_3 \rightarrow Y_2O_3(s) + 9\ CO + 28.5\ C_2H_2 \qquad (1b)$$

Rate constants and activation energies for both reactions are set to match literature[9] results by Pulver et al. for deposition of zirconia using low temperature (500-600°C) results. For both reactions the activation energy E_a is 83 kJ/mole and the pre-exponential is 10^5 m/s. This simple kinetics model (Model 1) does not consider any gas-phase reactions or reactions involving the solvent or oxygen carrier gas.

A second kinetics model (Model 2) includes the above precursor reactions with additional reactions involving pyrolysis of the solvent at the substrate surface.

$$C_4H_8O \rightarrow CO + CH_4 + C_2H_4 \qquad (2)$$

While the actual pyrolysis of THF is certainly more complex than (2) the essential feature of this reaction is the production of three moles of gas from one mole of THF. Other possible pyrolysis reactions will produce similar numbers of moles of gas. Solid carbon is not included as a product in this pyrolysis reaction. This is justified by experimental observation that the deposited films contained little or no carbon based on their white color and on minimal weight loss upon post-deposition heating in air. The rate constant for (2) is set arbitrarily to a value large enough to produce essentially complete reaction at the surface. The assumptions in this model are discussed below.

Fluid properties - viscosity and thermal conductivity - are set using Sutherland's law constants and Prandtl number for oxygen provided in the CFD-ACE properties database. Mass diffusivities for all gas-phase species, except the precursors, are calculated using Chapman-Enskog theory from Lennard-Jones parameters in the database. Precursor diffusivities are based on values for the Lennard-Jones parameters that were determined from vaporization rate data[10]. In calculating mass fluxes the Stefan-Maxwell equations are used to ensure species conservation.

RESULTS

Experiments at ORNL produced yttria-stabilized zirconia over a range of temperatures using direct liquid injection CVD. Model runs simulated these experiments using boundary conditions to match experimental process conditions.

EXPERIMENTAL RESULTS

Solubility experiments at ORNL showed a maximum solubility of $Zr(tmhd)_4$ in THF of 0.1 g/ml at room temperature. Preliminary CVD runs at this concentration produced intermittent clogging and stalling of the syringe pump and nebulizer used to deliver the liquid solution to the vaporization chamber. Subsequently all deposition experiments were run using a solution of 0.040 g/ml total precursor with a mixture of zirconia and yttria precursors at a metal ratio Y/(Y+Zr) of 0.165. Total solution flow was 0.87 ml/min with oxygen flow of 100 sccm. The nozzle (vaporizer) temperature was held at 200^{o}C and the substrate temperature ranged from 530 to 1100^{o}C for different runs.

YSZ deposit was confirmed by X-ray diffraction and scanning electron microscopy (SEM). Average deposit thickness was calculated from the weight gain of the substrate assuming fully dense YSZ. Under these gas flow and composition conditions, deposit thickness increases with increasing substrate temperature up to 925^{o}C and then decreases slightly.

Table 1. Summary of ORNL CVD results.

ORNL ID	Temperature (^{o}C)	Rate (μm/hr)
#16	530	0.38
#15	618	1.1
#13	710	3.7
#12	835	4.9
#11	925	7.4
#14	975	6.9
#10	1004	6.3
#17	1100	6.2

MODELING RESULTS

A series of model runs were conducted to simulate the above experiments. Boundary conditions were set to match ORNL experimental conditions as discussed above. Model runs provide both graphical and numerical output of system properties and deposition rate.

Representative model results are shown in Figure 2 as 2-D plots of temperature, axial (x) velocity and precursor concentrations. In the region between the inlet and the substrate, fluid flow and temperature profiles closely match those expected for ideal stagnation point flow, i.e. temperature and x-velocity are independent of radial position and depend only on height above the substrate surface. Near the outlet of the reactor the flow approaches fully developed, parabolic flow. Very slight recirculation zones are formed in the annular region outside of the nozzle. While velocity values change somewhat the overall flow profile is the same for all temperatures. Precursor concentrations above the substrate are independent of radial position and show nearly complete depletion of the precursors at the surface for temperatures above approximately 700^{o}C. Under these conditions the deposition rate is controlled by the rate of diffusion across a mass-transport pseudo-boundary layer that is approximately 0.35 cm wide.

Figure 3 shows the model-calculated deposition rate as a function of radial position for a substrate temperature of 710^{o}C. The rate is constant (+/- 0.6%) from the center of the substrate to a radius of about 1.0 cm, reflecting the near ideal stagnation point flow conditions. Beyond this radial position the deposition rate rises as the flow turns downward at the edge of the substrate holder. The yttria concentration in the film matches that in the mixed precursor solution. As shown in Figure 4 Model 1 results predict a deposition rate about twice that observed experimentally. Model 2 results are close to experiment at high temperatures. At low temperatures (less than 700^{o}C) this model predicts significantly higher deposition rate than observed experimentally.

DISCUSSION

Overall the model suggests that the reactor produces the stagnation point flow conditions that are desired from this reactor design. These conditions allow separation of the reaction kinetics and mass transport effects that jointly control the deposition rate. The transition from the "kinetics-limited" regime to the "mass-transport limited" regime appears to be approximately 700^{o}C in the model and somewhat higher in experiments. The highest deposition rates occur above this temperature and change only slightly with temperature up to 1100^{o}C. It is important to recognize that in this transport-limited regime the deposition rate is insensitive to the values of the surface reaction rate constants. For example, reducing the pre-exponential factor in the deposition rate constants for equations (1) and (1a) by a factor of ten produces only a 12% drop in calculated deposition rate at 1000^{o}C. In this regime the deposition rate depends primarily on the velocity profile (i.e. the thickness of the pseudo-boundary layer), the values of the precursor diffusion constants and the composition of the gas phase above the substrate.

The calculated deposition rate using Model 1 is significantly higher than that found experimentally. This model assumes that the THF solvent does not decompose within the reactor but rather behaves as an inert carrier gas. This assumption clearly is not valid near the substrate where temperatures are high enough to produce decomposition of any organic compound. The exact decomposition path likely involves many gas-phase and surface reactions, and is unknown. Even if the reaction mechanism were known, the associated reaction rate constants may not be available and incorporation of a multi-step pyrolysis reaction would complicate the model considerably.

Model 2 represents a limiting case for solvent pyrolysis. It assumes that ALL solvent molecules reaching the surface react to form small, stable products. Again, neither the exact mechanism of this reaction nor the distribution of products is known. However, stoichiometry places limits on the TOTAL number of moles of gaseous product that can be produced from one mole of solvent. For THF this limit is three and Model 2 builds this limit into the model. Calculated deposition rates including equation (2) are a close match to experiments at high temperatures suggesting that this assumption is reasonable. The reduction in deposition rate in the transport-limited regime is due to two effects: the increase in moles of "carrier" gas due to pyrolysis dilutes the precursor concentration at the surface and the net production of gas at the surface creates a flow away from the substrate that slows transport of precursor from outside the boundary layer. This "solvent effect" on CVD rate in direct liquid injection has not been recognized previously.

The model can be used to investigate the effect of pressure on the deposition rate. The pressure in all model runs was set at 2370 Pa (18 torr) which was the nominal pressure in early ORNL experiments. In some of the later runs the pressure control point was somewhat lower, 660-1320 Pa (5-10 torr). In actuality the pressure was somewhat variable throughout these experiments. However, the model indicates that deposition rate is independent of pressure within this range. For example, at 1004^{o}C, the calculated deposition rate is 4.71, 4.74 and 4.76 μm/hr at 1185, 2370 and 4740 Pa respectively. Although the gas phase concentration (moles/cm^2) of precursor is proportional to pressure, the inlet velocity is inversely proportional and these two terms cancel, leaving the deposition rate essentially independent of pressure.

Experiment and model result both show that YSZ deposition rate cannot be increased beyond 8-10 μm/hr by simply increasing the substrate temperature or by changing the pressure. The model suggests two other process changes that will increase deposition rate: increasing the solution delivery rate and increasing the precursor concentration. Increasing the solution delivery rate increases the molar flow and inlet velocity. This reduces the thickness of the mass transport pseudo-boundary layer, increasing the rate of precursor transport to the surface. Increasing the precursor concentration in solution increases the gas phase concentration in the reactor which increases the diffusive transport to the depleted substrate surface. Figure 5 shows the result of model calculations of deposition rate for a four-fold increase of solution flow rate and precursor concentration. The deposition rate is approximately proportional to the precursor concentration and to the square root of the flow rate.

FUTURE WORK

The YSZ model shows reasonably good match to experimental results for this simple reactor and substrate geometry. Future work will include refinement of the model to improve prediction of deposition rate, exploration of methods to increase the experimental deposition rate and incorporation of realistic turbine vane geometry into the model.

For reactor conditions that produce high deposition rates, gas phase transport – rather than surface kinetics – is always the limiting and controlling factor. While the present model includes full, multi-component transport there is some uncertainty about the values of key diffusion constants, particularly for the precursor species. Also, gas phase reactions are not included in the current model and these may be important at high temperature. Model refinements will be evaluated by comparison to future experiments at ORNL. Current results for YSZ are limited to one set of process conditions. Additional runs with different temperatures, precursor concentrations and flow conditions will guide model development.

High deposition rate is desirable for a commercial CVD process. Previous studies and these modeling results clearly show that gas phase mass transport is the limiting factor at high deposition rates. Under these conditions the gas phase concentration of the precursor at the inlet and the mass diffusivity of the precursor are rate-controlling factors. With the ORNL reactor the gas phase concentration is limited by the choice of precursor and its solubility in the selected solvent for the direct liquid delivery system. Additional precursor-solvent combinations will be evaluated to identify combinations that will provide increased gas phase precursor concentration in the reactor. The gas phase mass diffusivity of a molecular species depends on its molecular weight and size and on the characteristics of the other species in the mixture. Candidate precursor-solvent combinations will be evaluated with respect to increasing the diffusion rate of precursor to the surface.

The ultimate goal of this research program is to develop a precise tool for design of a CVD reactor for applying a thermal barrier coating to fossil energy system components. With success in modeling the simple ORNL stagnation point flow reactor, the next step is to incorporate realistic turbine vane geometry into the model and use the model to explore reactor modifications that produce desirably uniform YSZ coatings.

ACKNOWLEDGEMENT

The experimental results shown in this report were obtained at Oak Ridge National Laboratory by Mr. Venu Veranasi under the direction of Dr. Theodore Besmann. Their timely communication of these results has been invaluable in development of an accurate process model.

REFERENCES

1. J. Minet, F. Langlais and R. Naslain, “On the chemical vapour deposition of zirconia from $ZrCl_4$-H_2-CO_2-Ar gas mixture: II. An experimental approach,” Journal of the Less-Common Metals 132 (1987) 273-287
2. E. Sipp, F. Langlais and R. Naslain, “CVD of yttria from YCl_3-CO_2-H_2-Ar gas mixture: an experimental study,” Journal of Alloys and Compounds 186 (1992) 77-87
3. E. Sipp, F. Langlais and R. Naslain, “Kinetics of deposition of zirconia-based ceramics from $ZrCl_4$- H_2- CO_2-Ar gas mixtures,” Journal of Alloys and Compounds 186 (1992) 65-76)
4. T. Belmonte, J. Gavillet, T. Czerwiec, D. Ablitzer and H. Michel, “Hydrodynamic and Chemical Modeling of a Chemical Vapor Deposition Reactor for Zirconia Deposition,” J.Phys.III France 7 (1997) 1779-1796
5. J. Gavillet, T. Belmonte, D. Hertz and H. Michel, “Low temperature zirconia thin film synthesis by a chemical vapour deposition process involving $ZrCl_4$ and O_2-H_2-Ar microwave post-discharges. Comparison with a conventional CVD hdrolysis process,” Thin Solid Films 301 (1997) 35-44
6. Masanobu Aizawa, Chihiro Kobayashi, Hisanori Yamane and Toshio Hirai, “Preparation of ZrO2-Y2O3 films by CVD using β-diketone metal chelates” Journal of the Ceramic Society of Japan, International Edition, 101 (1993) 283-286
7. Sang-Chul Hwang and Hyung-Shik Shin, “Effect of deposition temperature on the growth of yttria-stabilized zirconia thin films on Si(111) by chemical vapor deposition” Journal of the American Ceramic Society 82 (1999) 2913-2915
8. Jesus J. Gallegos III, Timothy L. Ward, Timothy J. Boyle, Mark A. Rodriguez and Laila P Francisco, “Neo-pentoxide precursors for MOCVD thin films of TiO2 and ZrO2” Advanced Materials 12 (2000) 21-26
9. M. Pulver, W. Nemetz and G. Wahl, “CVD of ZrO_2, Al_2O_3 and Y_2O_3 from metal-organic compounds in different reactors,” Surface and Coatings Technology 125 (2000) 400-406
10. M. Pulver, G. Wahl, H. Scheytt and M. Sommer, “Deposition of ZrO_2 and Y_2O_3-stabilized ZrO_2 from β-diketonates,” Journal de Physique II-C3 3 (1993) 305-312
11. C. Dubourdieu, S.B. Kang, Y.Q. Li, G. Kulesha and B. Gallois, “Solid single-source metal organic chemical vapor deposition of yttria-stabilized zirconia” Thin Solid Films 339 (1999) 165-173
12. I.S. Chuprakov, J.D. Martin and K.H. Dahmen, “New flash-evaporation feeder for chemical vapor deposition” Journal De Physique. IV 9 (1999) Pr8-901 - Pr8-908
13. Anthony C. Jones, Timothy J. Leedham, Peter J. Wright, Michael J. Crosbie, Dennis J. Williams, Kirsty A. Fleeting, Hywel O. Davies, David J. Otway and Paul O'Brien, “Liquid injection MOCVD of zirconium dioxide using a novel mixed ligand zirconium precursor” Advanced Materials 10 (1998) 197-201
14. Susan Krumdieck and Rishi Raj, “Conversion efficiency of alkoxide precursor to oxide films grown by an ultrasonic-assisted, pulsed liquid injection, metalorganic chemical vapor deposition (pulsed-CVD) process” Journal of the American Ceramic Society 82 (1999) 1605-1607
15. H.B. Wang, C.R. Xia, G.Y. Meng and D.K. Peng, “Deposition and characterization of YSZ thin films by aerosol-assisted CVD” Materials Letters 44 (2000) 23–28
16. T. M. Besmann, V. Varanasi, T. J. Anderson, T. L. Starr and W. Xu, “Chemically Vapor Deposited YSZ for Thermal and Environmental Barrier Coatings”, 16th Annual Conference on Fossil Energy Materials, April 22-24, 2002 http://www.netl.doe.gov

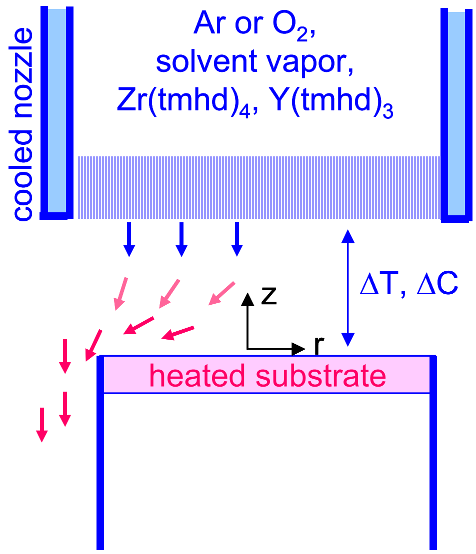

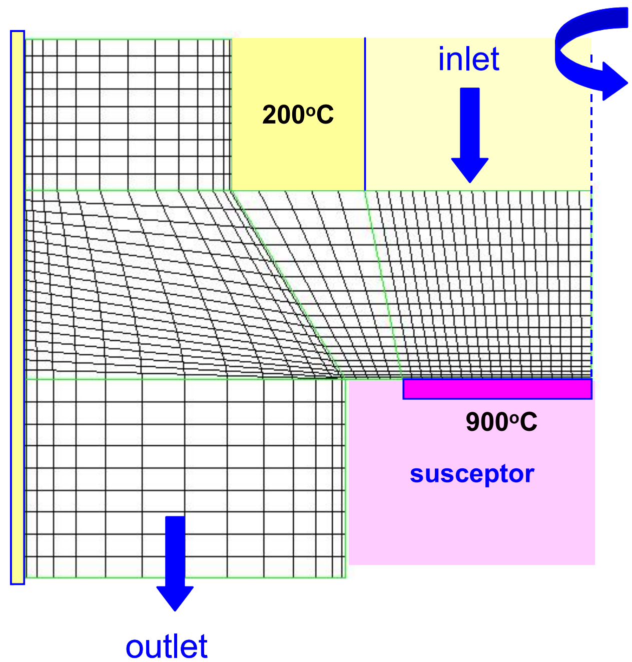

Figure 1. ORNL reactor (left) uses a stagnation point flow configuration. CVD model for this reactor uses a variable mesh and boundary conditions as shown (right).

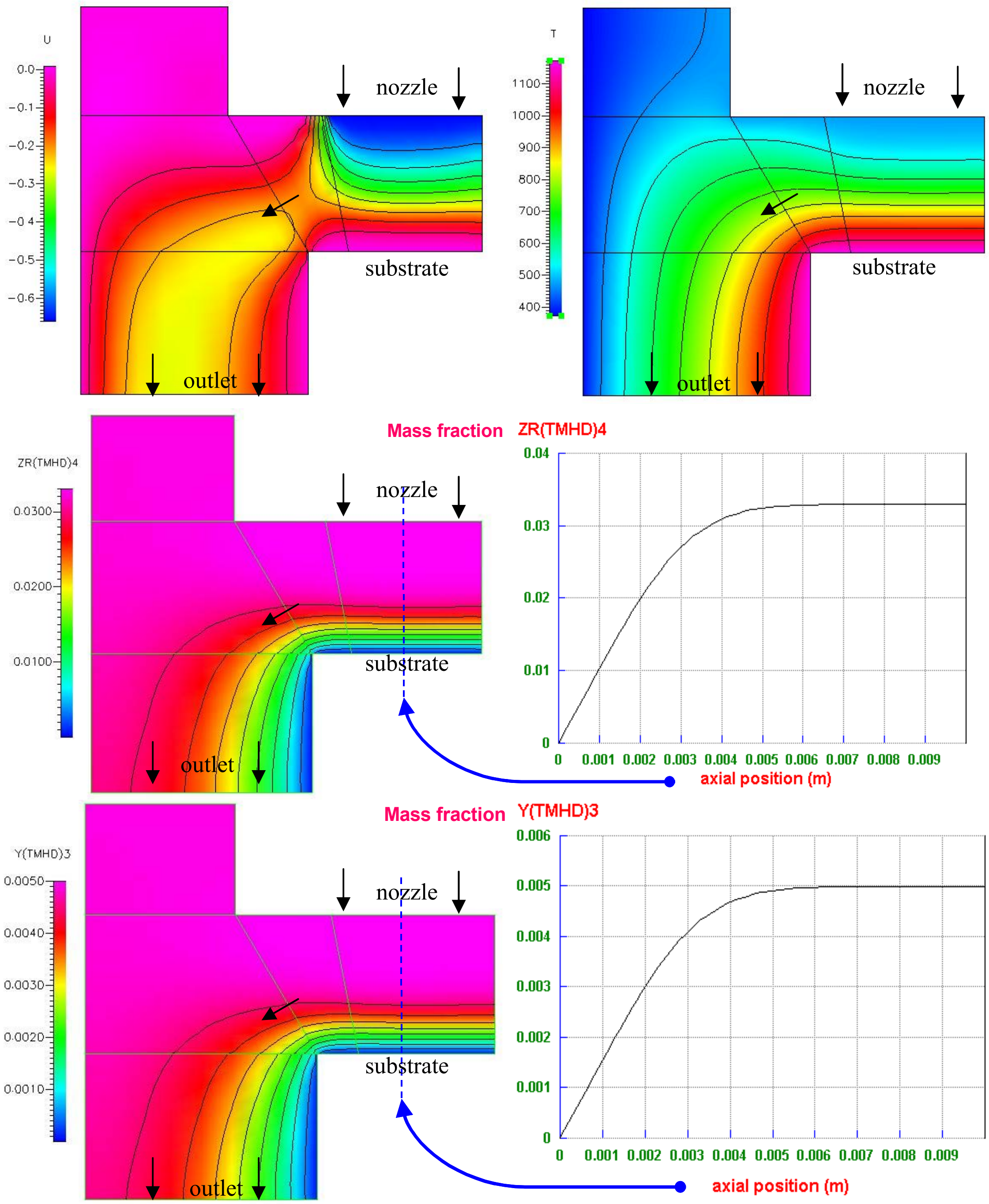

Figure 2. Plots of axial velocity (units = m/s, top left) and temperature (units = K, top right) show that these quantities are approximately independent of radial position in the region between the nozzle and substrate. Depletion of $Zr(tmhd)_4$ (middle plots) and $Yr(tmhd)_3$ (bottom plots) at substrate indicates that deposition rate is limited by diffusion across a mass transfer boundary of approximately 3.5 mm width.

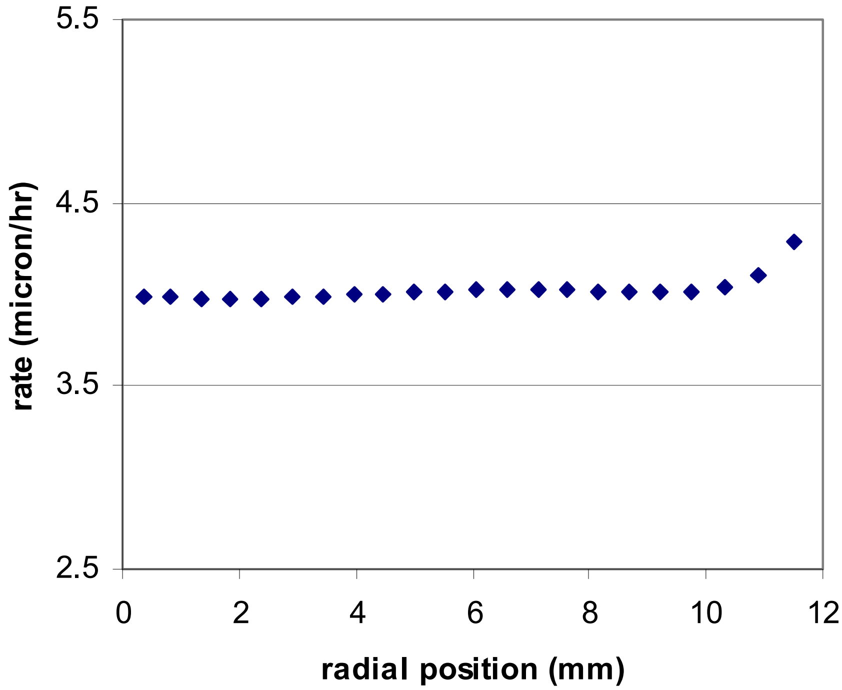

Figure 3. Model including solvent pyrolysis (Model 2) predicts uniform deposition rate (+/- 0.6%) within 1.0 cm of the center of the substrate. For these conditions, ORNL observed a deposition rate of 3.7 micron/hr.

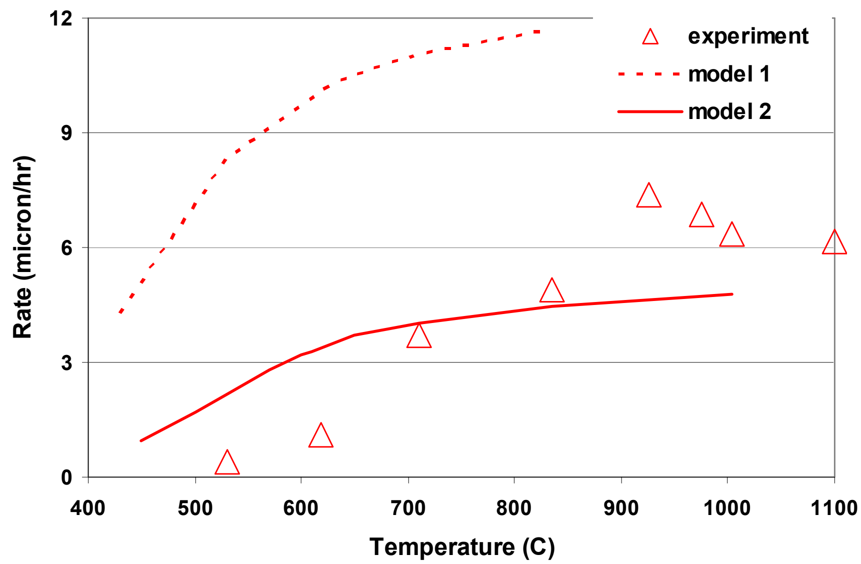

Figure 4. Calculated deposition rate without (Model 1) and with (Model 2) solvent pyrolysis is compared to ORNL experimental results. Pulver results (reference) are shown for comparison.

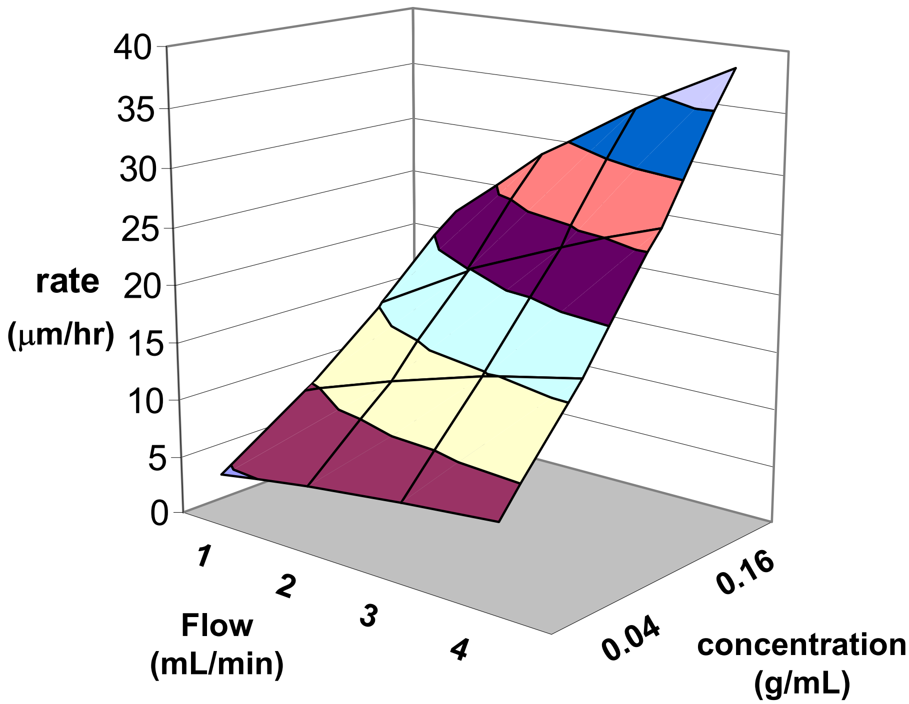

Figure 5. Deposition rate increases with increasing solution flow rate and with increasing concentration of precursor in the solution.